Natural Science, 2014, 6, 262-277
Published Online March 2014 in SciRes. http://www.scirp.org/journal/ns
http://dx.doi.org/10.4236/ns.2014.65030

Scientific Research

Mathematical Model of Cell Growth for Biofuel Production under Synthetic Feedback

Ondivillu Mothilal Kirthiga, Lakshmanan Rajendran

Department of Mathematics, The Madura College, Madurai, India
Email: raj_sms@rediffmail.com

Received 10 January 2014; revised 10 February 2014; accepted 17 February 2014

Abstract

In this paper, mathematical model for cell growth and biofuel production under synthetic feedback loop is discussed. The nonlinear differential equations are solved analytically for the maximum production of biofuel under synthetic feedback. The closed-form of analytical expressions pertaining to the concentrations of cell density, repressor proteins, pump expressions, intracellular biofuel and extracellular biofuel are presented. The constant pump model is compared with feedback loop model analytically to know the biofuel production. The numerical solution of this problem is also reported using Scilab/Matlab program. Also, the analytical results are compared with previous published numerical results and found to be in good agreement.

Keywords

Mathematical Modeling; Non-Linear Equations; Biofuel; Feedback Loop; Biosensor

1. Introduction

Micro-organisms (or microbes) play a very important role in our lives. Some microbes cause disease but the majority is completely harmless. Microbes help as for the production of enzymes and chemicals. In particular, most common biofuel is ethanol, which is produced from the plants. Breakdown of cellulous will also form ethanol. However, there are numerous scientific and technical challenges involved with utilizing lignocelluloses material for biofuel production.

Biological and biochemical processes have a very important role in medicine, biology and biotechnology. However, it is very difficult to convert directly biological data to electrical signal; the biosensors can convert these signals and the biosensors over this difficulty [1]. The advantages of biosensors such as cost-effectiveness,

How to cite this paper: Kirthiga, O.M. and Rajendran, L. (2014) Mathematical Model of Cell Growth for Biofuel Production under Synthetic Feedback. *Natural Science*, **6**, 262-277. http://dx.doi.org/10.4236/ns.2014.65030

specificity of detection, portability reduced overall time required for detection. Clark *et al*. [2] developed the first biosensor, an enzyme based glucose sensor. Then so many biosensors are developed in many research laboratories [3].

The cell growth and biofuel production implement a synthetic feedback loop using a biosensor to control efflux pump expression. In this way, the production rate will be maximal when the concentration of biofuel is low because the cell does not expend energy expressing efflux pumps when they are not needed. Efflux pumps identify harmful compounds; transfer them from the cell using the proton motive force and have proven effective at exporting biofuel. Even though they improve tolerance, if over expressed, efflux pumps can be harmful. By using efflux pumps giving to increase tolerance to biofuel, pump toxicity managed biofuel toxicity. Feedback is a common mechanism to adjust the conditions such as environmental stressors and signals from other cells. Synthetic feedback helps to control efflux pump expression which would balance the toxicity of biofuel production against the adverse effect of pump expression.

Clomburg *et al*. [4] discussed that synthetic biology will help improve the productivities of biofuels. The mechanism of microbes causes unwanted cellulose stress that leads to over production of proteins which results in decreases of cell fitness. Fisher *et al*. [5] tested seven fast growing host organisms for biofuel production which tolerate production stresses. Mostafa *et al*. [6] provided a brief overview on the research in the area of biofuels, with specific emphasis on the economic viability of various approaches.

Peralta *et al*. [7] concentrated on the metabolic engineering of genetically polite organisms such as *Escherichia coli* and *Saccharomyces cerevisiae* for the production of these advanced biofuels. Soto *et al*. [8] studied the importance of efflux pumps in biofilm growth and about their relevance in antimicrobial resistance forming biofilm. Huffer *et al*. [9] highlighted recent advances in metabolic engineering of biofuel-synthesis pathways in *E. coli* and summarized insights gained into regulation of those pathways, and described progress toward overcoming the challenges facing its adoption as a biofuel-production strain. Christopher *et al*. [10] discussed the contributions of systems biology for the purpose of utilizing microorganisms for biofuel production.

Recently, Dunlop *et al*. [11] developed a model for cell growth and biofuel production. Harrison *et al*. [12] developed a mathematical model for cell growth and biofuel production that implement a synthetic feedback loop using a biosensor to control efflux pump expression. To the best of our knowledge, there is no general analytical expression for the concentration of cell density, repressor proteins, pump expressions, intracellular biofuel and extracellular biofuel against the time *t*. The purpose of this paper is to derive an analytical expression for the concentrations of cell density, repressor proteins, pumps, intracellular biofuel and extracellular biofuel for both steady and non-steady state conditions.

2. Mathematical Formulation of the Problem

2.1. Feedback Loop Model

The complete mathematical formulation of this problem is described in [12]. This model involves five nonlinear differential equations with limited number of parameter are described as follows [12]:

$$\frac{\mathrm{d}n(t)}{\mathrm{d}t} = \alpha_n n(t)\left(1-\frac{n(t)}{n_{\max}}\right) - \delta_n b_i(t) n(t) - \frac{\alpha_n p(t) n(t)}{p(t)+\gamma_p} \tag{1}$$

$$\frac{\mathrm{d}R(t)}{\mathrm{d}t} = \alpha_R + k_R\left(\frac{I}{I+\gamma_I}\right) - \beta_R R(t) \tag{2}$$

$$\frac{\mathrm{d}p(t)}{\mathrm{d}t} = \alpha_p + k_p \frac{1}{\left[R(t)/\left(1+k_b b_i(t)\right)\right]+\gamma_R} - \beta_p p(t) \tag{3}$$

$$\frac{\mathrm{d}b_i(t)}{\mathrm{d}t} = \alpha_b n(t) - \delta_b p(t) b_i(t) \tag{4}$$

$$\frac{\mathrm{d}b_e(t)}{\mathrm{d}t} = v\delta_b p(t) b_i(t) n(t) \tag{5}$$

Here $n(t), R(t), p(t), b_i(t)$ and $b_e(t)$ denote concentrations of cell density, repressor proteins, pumps,

intracellular biofuel and extracellular biofuel respectively. Delay in cell growth is happens due to biofuel toxicity $(\delta_n b_i n)$ and pump toxicity $\alpha_n np/(p+\gamma_p)$. When the promoter is not activated, α_R and α_p represents the low level of expression. β_p and β_R represent the degradation rates. k_R and k_p represent the strength of expression for R and p, respectively. In Equation (3), $1/(R/(1+k_b b_i)+\gamma_R)$ represents the repression of efflux pump expression and $R/(1+k_b b_i)$ represents the amount of active R in the system. The parameter k_b represents the deactivation constant of R. Repressor activation by the inducer IPTG is modeled as $I/(I+\gamma_I)$, where γ_I indicates the inducer value that corresponds to half maximal activation of repressor. Amount of inducer is proposional to the repressor concentration. The initial conditions are given by.

$$\text{At } t=0, n(t)=n_0, R(t)=R_0, p(t)=p_0, b_i(t)=b_{i0}, b_e(t)=b_{e0} \tag{6}$$

The steady state expressions of the concentrations for this model are obtained as follows:

$$n_s=\frac{n_{\max}}{\alpha_n}\left[\alpha_n-\delta_n J-\alpha_n p_s\left(\frac{1}{p_s+\gamma_p}\right)\right] \tag{7}$$

$$R_s=\frac{1}{\beta_R}\left[\alpha_R+k_R\left(\frac{I}{I+\gamma_I}\right)\right] \tag{8}$$

$$p_s=\frac{R_s\alpha_p+\alpha_p\gamma_p+k_p+\left(\alpha_p\gamma_p k_b+k_b k_p\right)J}{\beta_p(\gamma_R+R_s)+\left(\beta_p\gamma_p k_b\right)J} \tag{9}$$

$$b_{is}=\frac{\alpha_b n_{\max}}{\alpha_n\delta_b p_s}\left[\alpha_n-\delta_n J-\alpha_n p_s\left(\frac{1}{p_s+\gamma_p}\right)\right] \tag{10}$$

where $J=\frac{K^{1/3}}{6E}-\frac{2\left(3GE-F^2\right)}{3EK^{1/3}}-\frac{F}{3E}$,

$K=36GFE+108HE^2-8F^3+12\sqrt{3}\sqrt{4G^3E-G^2F^2+18EFGH+27H^2E^2-4EHF^3}$

and other parameters are in **Table 1**.

Analytical Expressions of the Concentrations of Cell Density, Repressor Proteins, Pumps, Intracellular and Extracellular Biofuel

By solving the non-linear Equations (1)-(5) using Homotopy perturbation method (**Appendix A**) [13]-[18], the analytical expressions of the concentrations of cell density, repressor proteins, pumps, intracellular and extracellular biofuel are obtained for non-steady state as follows:

$$n(t)=\frac{L}{\frac{\alpha_n}{n_{\max}}+\frac{1}{n_0}\left(L-\frac{n_0\alpha_n}{n_{\max}}\right)e^{-Lt}} \tag{11}$$

$$R(t)=R_s+e^{-\beta_R t}\left(R_0-R_s\right) \tag{12}$$

$$p(t)=\frac{1}{\beta_p}\left\{\alpha_p+\frac{k_p}{\left(R_s/(1+k_b b_s)\right)-\gamma_R}+e^{-\beta_p t}\left[\beta_p p_0-\alpha_p-\frac{k_p}{\left(R_s/(1+k_b b_s)\right)-\gamma_R}\right]\right\} \tag{13}$$

$$b_i(t)=\frac{\alpha_b n_s+e^{-\delta_b p_s t}\left(\delta_b p_s b_{io}-\alpha_b n_s\right)}{\delta_b p_s} \tag{14}$$

$$b_e(t)=b_{eo}+\frac{n_{\max}v\delta_b p_s b_{is}}{\alpha_n}\left\{\ln\left[\frac{n_s\alpha_n}{Ln_{\max}}\left(1-e^{-Lt}\right)+e^{-Lt}\right]+Lt\right\} \tag{15}$$

where

$$L=\left(\alpha_n-\delta_n b_{is}-\frac{\alpha_n p_s}{p_s+\gamma_p}\right) \tag{16}$$

Table 1. Symbols used.

Symbols	Definitions	Values	Units
b_e	Concentration of extracellular biofuel	-	None
b_{e0}	Initial concentration of extracellular biofuel	0	None
b_i	Concentration of intracellular biofuel	-	M
b_{is}	Steady state of intracellular biofuel (feedback loop model)	-	M
b_{is1}	Steady state of intracellular biofuel (constant pump model)	-	M
b_{i0}	Initial concentration of intracellular biofuel	0	M
I	IPTG level	0 - 1	mM
k_b	Repressor deactivation constant	100	M^{-1}
k_p	Pump activation constant	0.2	h^{-1}
k_R	Repressor activation constant	10	h^{-1}
n	Concentration of cell density	-	None
n_s	Steady state expressions of cell density (feedback loop model)	-	None
n_{s1}	Steady state expressions of cell density (constant pump model)	-	None
n_{max}	Maximum population size	1	None
n_0	Initial concentration of cell density	0.01	None
p	Concentration of pump expressions	-	None
p_s	Steady state expression of pumps (feedback pump model)	-	None
p_{s1}	Steady state expression of pumps (constant pump model)	-	None
p_0	Initial concentration of pump expressions	0	None
R	Concentration of repressor proteins	-	None
R_s	Steady state expression of repressor proteins	-	None
R_0	Initial concentration of repressor proteins	0	None
t	Time	-	h^{-1}
Greek Letters			
α_b	Biofuel production rate	0.1	h^{-1}
α_n	Cell growth rate	0.66	h^{-1}
α_p	Basal pump production rate	0.01	h^{-1}
α_R	Basal repressor production rate	0.01	h^{-1}
β_p	Pump degradation rate	0.66	h^{-1}
β_R	Repressor degradation rate	2.1	h^{-1}
γ_I	Inducer saturation threshold	60	μM
γ_p	Pump toxicity threshold	0.14	none
γ_R	Repressor saturation threshold	1.8	none
δ_b	Biofuel export rate per pump	0.5	$M^{-1}{\cdot}h^{-1}$
δ_n	Biofuel toxicity coefficient	0.91	$M^{-1}{\cdot}h^{-1}$
v	Ratio of intra to extracellular volume	0.01	none
Subscripts			
b	Biofuel		
e	Extracellular biofuel		
i	Intracellular biofuel		
I	Inducer		
max	Maximum		

Continued

n	Cell density
p	Pump expressions
R	Repressor proteins
s	Steady state
Parameters	
$A = R_s\alpha_p + \alpha_p\gamma_b + k_p$	h^{-1}
$B = \alpha_p\gamma_R k_b + k_b k_p$	$M^{-1}\cdot h^{-1}$
$C = \beta_p\left(\gamma_R + R_s\right)$	h^{-1}
$D = \beta_p\gamma_R k_b$	$M^{-1}\cdot h^{-1}$
$E = mBD + uB^2 + qD^2$	$M^{-4}\cdot h^{-3}$
$F = mBC + mAD + 2uAB + 2qDC - lD^2$	$M^{-3}\cdot h^{-3}$
$G = mAC + uA^2 + Cq^2 - 2lCD$	$M^{-2}\cdot h^{-3}$
$H = lC^2$	$M^{-1}\cdot h^{-3}$
$l = \dfrac{\alpha_n\delta_b\gamma_p}{\alpha_b}$	$M^{-1}\cdot h^{-1}$
$L = \left(\alpha_n - \delta_n b_{is} - \dfrac{\alpha_n p_s}{p_s + \gamma_p}\right)$	h^{-1}
$m = \dfrac{\alpha_n\delta_b^2\gamma_p}{\alpha_b^2 n_{\max}} + \dfrac{\delta_b\delta_n}{\alpha_b}$	$M^{-2}\cdot h^{-1}$
$M = \left(\alpha_n - \delta_n b_{is1} - \dfrac{\alpha_n p_{s1}}{p_{s1} + \gamma_p}\right)$	h^{-1}
$q = \dfrac{\delta_n\delta_b\gamma_p}{\alpha_b}$	$M^{-2}\cdot h^{-1}$
$u = \dfrac{\alpha_n\delta_b^2}{\alpha_b^2 n_{\max}}$	$M^{-2}\cdot h^{-1}$

The Equations (11)-(15) represent new analytical expressions for the concentrations of cell density, pumps, intracellular and extracellular biofuel for this model.

2.2. Constant Pump Model

For this model, the concentration of repressor proteins $R(t)$ is removed and the concentration of cell density $n(t)$, intracellular biofuel $b_i(t)$ and extracellular biofuel $b_e(t)$ remains the same. But the concentration of pumps expression $p(t)$ becomes

$$\frac{\mathrm{d}p(t)}{\mathrm{d}t} = \alpha_p + k_R\left(\frac{I}{I+\gamma_I}\right) - \beta_p p(t) \tag{17}$$

where the value of I (IPTG) is selected from 0 mM to 1 mM. We can obtain the steady state expressions of concentrations for constant pump model as follows:

$$p_{s1} = \frac{1}{\beta_p}\left[\alpha_p + k_R\left(\frac{I}{I+\gamma_I}\right)\right] \tag{18}$$

$$b_{is1} = \frac{\alpha_n \alpha_b n_{\max} \gamma_p}{\left(p_{s1} + \gamma_p\right)\left(\alpha_b \delta_n n_{\max} + \alpha_n \delta_b p_{s1}\right)} \tag{19}$$

$$n_{s1} = \frac{p_{s1} \delta_b b_{is1}}{\alpha_b} \tag{20}$$

Analytical Expressions of the Concentrations of Cell Density, Pumps, Intracellular and Extracellular Biofuel

By solving the Equations (1), (4), (5) and (17), the closed form of an analytical expression of the concentrations of pumps, intracellular biofuel and extracellular biofuel are obtained as follows:

$$n(t) = \frac{M}{\frac{\alpha_n}{n_{\max}} + \frac{1}{n_0}\left(M - \frac{n_0 \alpha_n}{n_{\max}}\right)\mathrm{e}^{-Mt}} \tag{21}$$

$$p(t) = p_s + \mathrm{e}^{-\beta_p t}\left(p_0 - p_s\right) \tag{22}$$

$$b_i(t) = \frac{1}{\delta_b p_{s1}}\left[\alpha_b n_{s1} + \mathrm{e}^{-\delta_b p_{s1} t}\left(\delta_b p_{s1} b_{io} - \alpha_b n_{s1}\right)\right] \tag{23}$$

$$b_e(t) = b_{eo} + \frac{v \delta_b p_{s1} b_{is1}}{\alpha_n}\left\{\ln\left[\frac{n_{s1}\alpha_n}{M n_{\max}}\left(1 - \mathrm{e}^{-Mt}\right) + \mathrm{e}^{-Mt}\right] + Mt\right\} \tag{24}$$

where

$$M = \left(\alpha_n - \delta_n b_{is1} - \frac{\alpha_n p_{s1}}{p_{s1} + \gamma_p}\right) \tag{25}$$

The Equations (21)-(24) represents new analytical expressions for the concentrations of cell density, pumps, intracellular and extracellular biofuel for constant pump model.

3. Numerical Simulation

The non-linear differential Equations (1)-(5) are solved by numerical method. The function pdex4 in Scilab software which is a function of solving partial differential equations (PDE) is used to solve these equations. To show the efficiency of the present method, our analytic results are compared with numerical solution and it gives a satisfactory agreement. The SCILAB/MATLAB program is also given in **Appendix B**.

4. Discussion

Equations (11)-(15) represents simple analytical expressions for the concentrations of cell density, pumps, intracellular and extracellular biofuel in terms of six parameters, biofuel export rate δ_b, biofuel toxicity coefficient δ_n, biofuel production rate α_b, growth rate α_n, pump toxicity threshold δ_p, and maximum cell density $n_{\max}$. Those parameters give the greatest impact on the system when they are varied. Production of biofuel depends upon the growth rate, maximum cell density, pump toxicity threshold and biofuel toxicity coefficient.

Simulation results are often used to validate the analytical solutions. Recently, Harrison *et al*. [12] obtained the numerical solution of the nonlinear equations in feedback model using MATLAB program. The **Figure 1** shows cell density $n(t)$, pump $p(t)$, intracellular biofuel $b_i(t)$, extracellular biofuel $b_e(t)$ versus time t. In this figure, our analytical results are compared with the simulation results. Our analytical results were found to be in satisfactory agreement with simulation results.

Figure 2 represents the cell density $n(t)$ versus time *t*. The concentration depends upon the pump toxicity threshold γ_p, biofuel toxicity coefficient δ_n, maximum population size $n_{\max}$ and growth rate α_n. After very short time, cell density increases sharply and reaches the maximum value nearly 0.4 after 25 hours. Also from this figure, it is including that the cell density increases when growth rate is decreases and coefficient of biofuel toxicity is increases.

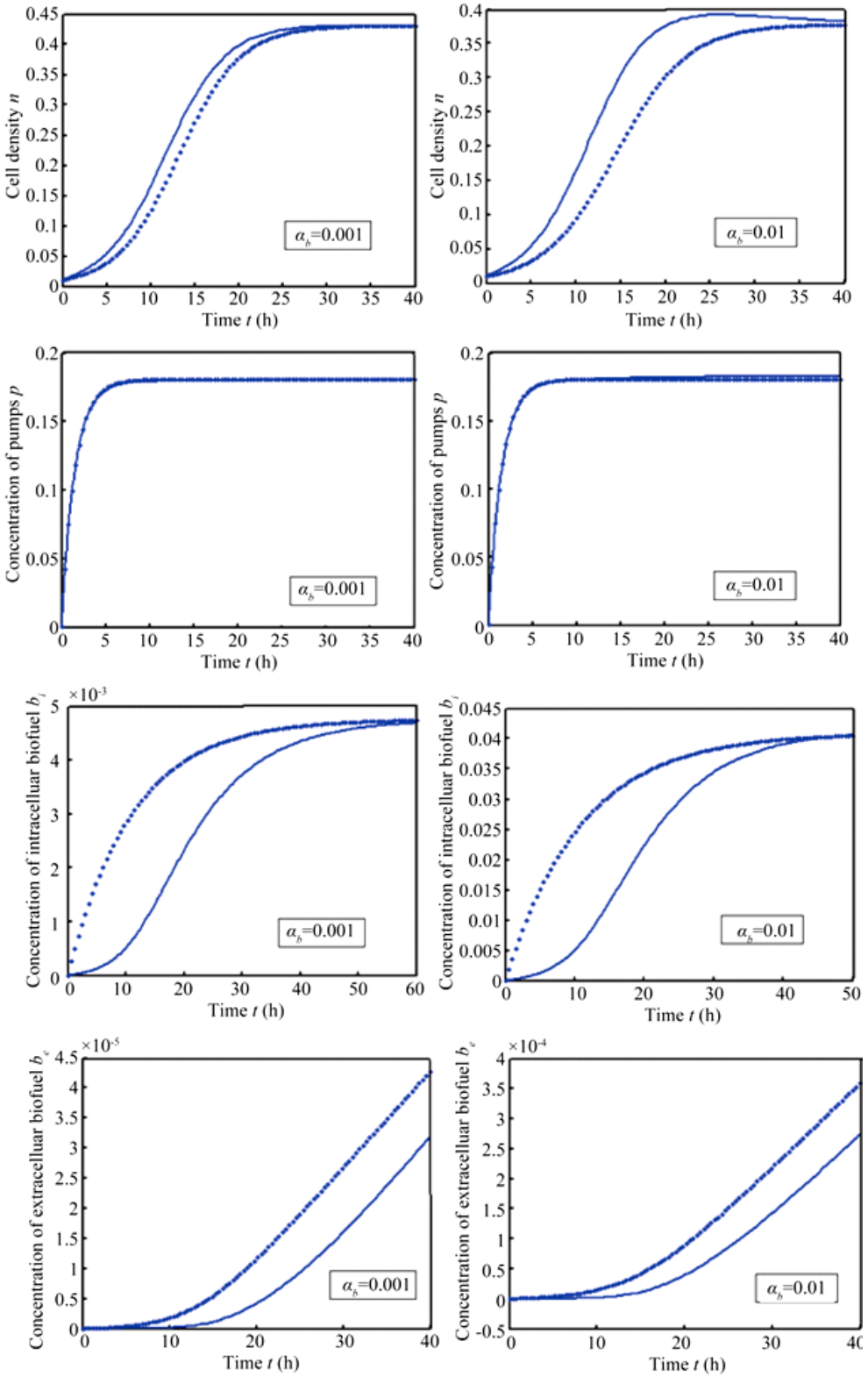

Figure 1. Comparison of analytical results (feedback model) with previous numerical results (Harrison *et al*., [12]): The concentrations were computed using Equations (11)-(15) for the experimental values. The key to the graph: dotted line represents the analytical results and solid line represents the numerical results.

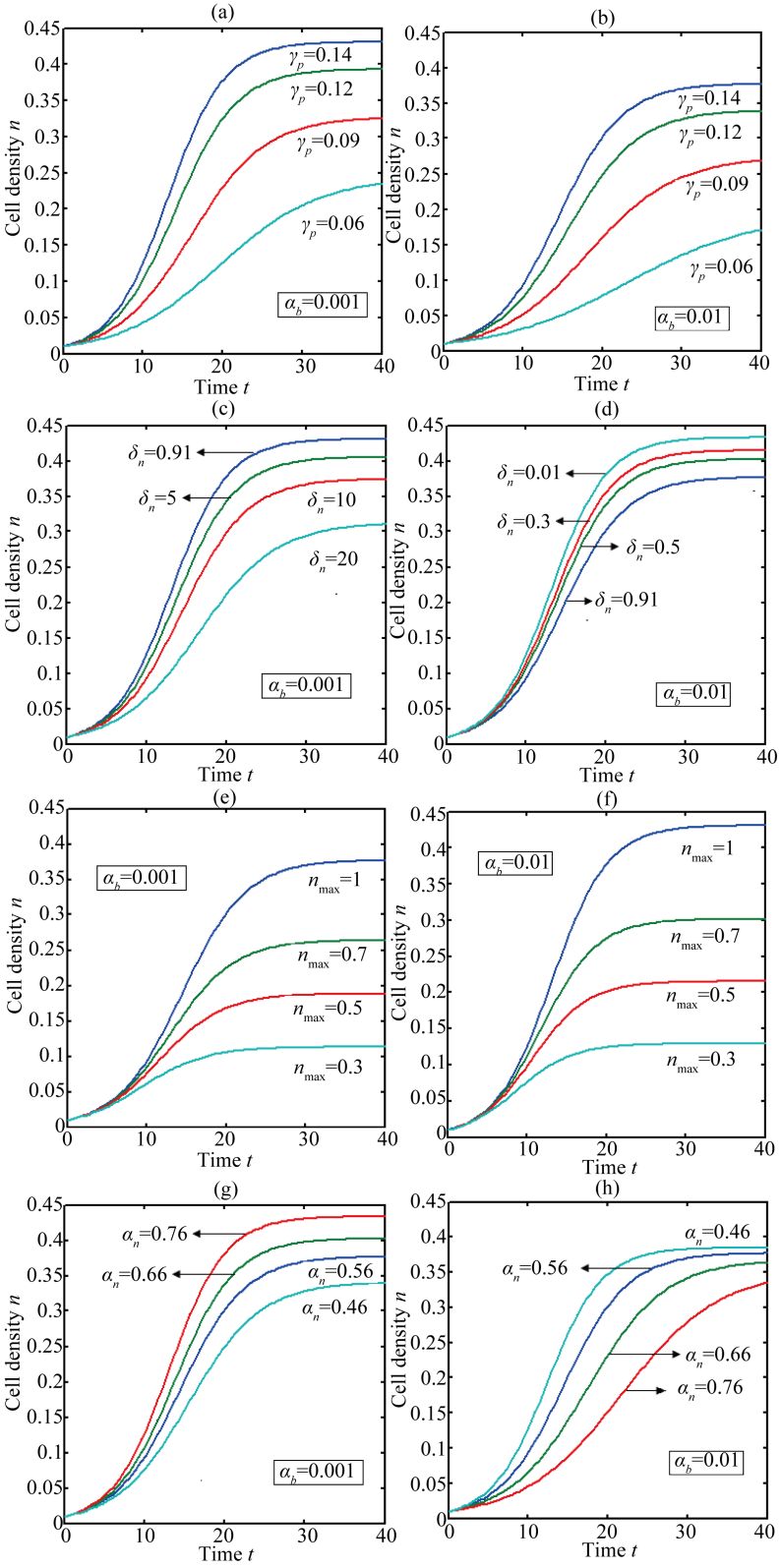

Figure 2. Cell density $n(t)$ versus time t for various values of pump toxicity threshold γ_p, biofuel toxicity coefficient δ_n, maximum population size n_{max} and growth rate α_n and for some fixed values of the parameters (refer **Table 1**).

The concentration of repressor $R(t)$ with time t for various values of repressor degradation rate β_R, repressor activation constant k_R and basal repressor production rate α_R is shown in **Figure 3**. When time increases the concentration also increases and finally it reaches the steady state value at short time $t = 2$. Repressor prevents efflux pump expression until it is deactivated by biofuel.

In **Figure 4**, the concentration of pumps $p(t)$ measured with time t for various experimental values of repressor saturation threshold γ_R, pump activation constant k_p, pump degradation rate β_p and basal pump production rate α_p. If time increases the concentration also increases and finally it reach steady state level by the control of efflux pump using feedback model. Pump expression increases the biofuel productions because of repressor deactivation. Concentration of pump depends upon the rate of pump expression.

Figure 5 describes the intracellular biofuel $b_i(t)$ with time t. For both biofuel production rate, when time t increases concentration of intracellular biofuel also increases. Biofuel rate is increased because intracellular biofuel accumulates more quickly and efflux pumps are needed earlier.

Figure 6 indicates the extracellular biofuel $b_e(t)$ versus time t. The concentration depends upon biofuel export rate per pump δ_b, ratio of intra to extracellular volume ν and cell growth rate α_n. For both biofuel production rate, if time increases the concentration also increases. From this figure, it is observed that the concentration of extracellular biofuel linearly increases with time t. This is because when efflux pumps are used to export biofuel form the cell the extracellular level of biofuel will increase, allowing intracellular biofuel levels to remain low.

An analytical expression of cell density $n(t)$, concentration of pump $p(t)$, intracellular biofuel $b_i(t)$ and extracellular biofuel $b_e(t)$ for feedback and constant pump model are compared in **Figure 7**. This figure

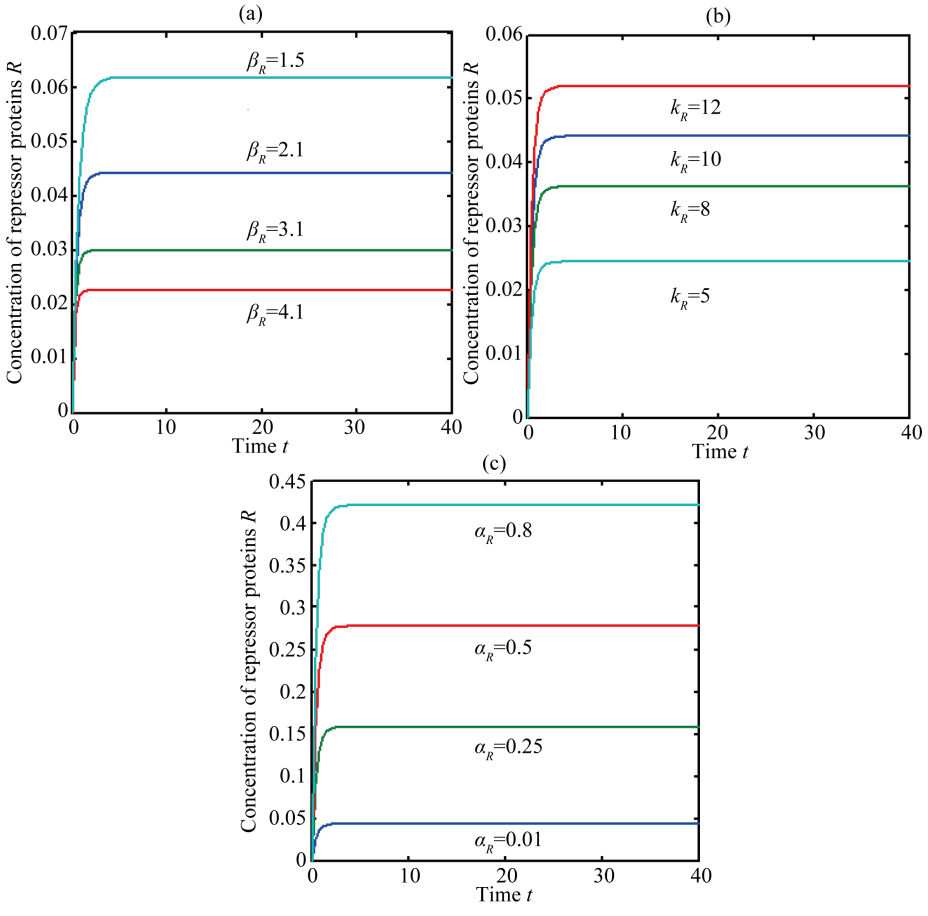

Figure 3. Concentration of repressor proteins $R(t)$ versus time t for various values of repressor degradation rate β_p, repressor activation constant k_R and basal repressor production rate α_R and for some fixed values of the parameters (refer **Table 1**).

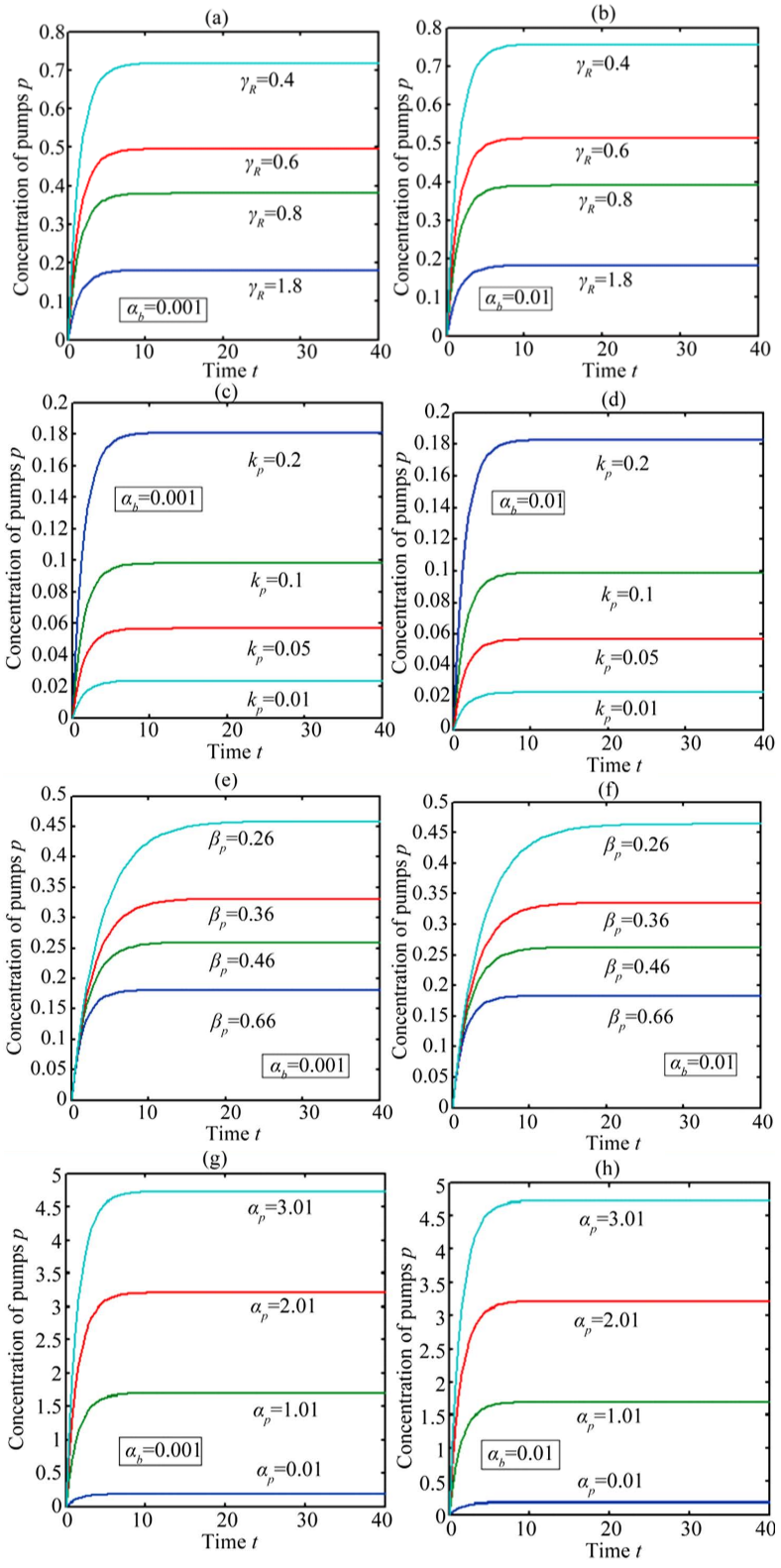

Figure 4. Concentration of pumps $p(t)$ versus time t for various values of repressor saturation threshold γ_R, pump activation constant k_p, pump degradation rate β_p and basal pump production rate α_p and for some fixed values of the parameters (refer **Table 1**).

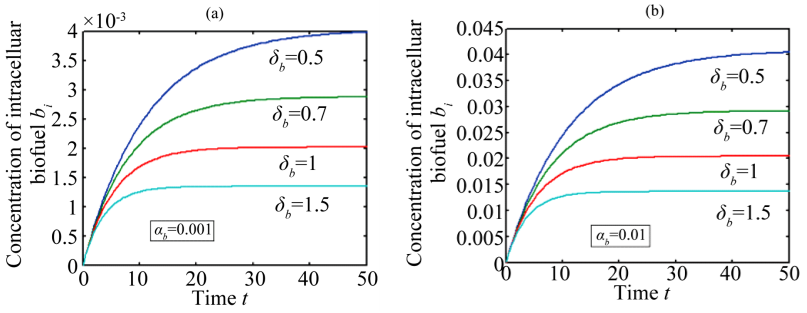

Figure 5. Concentration of intracellular biofuel $b_i(t)$ versus time t (a) At α_b = 0.001 for various values of biofuel export rate per pump δ_b and some fixed experimental values of other parameters. (b) At α_b = 0.01 for various values of δ_b and some fixed experimental values of other parameters.

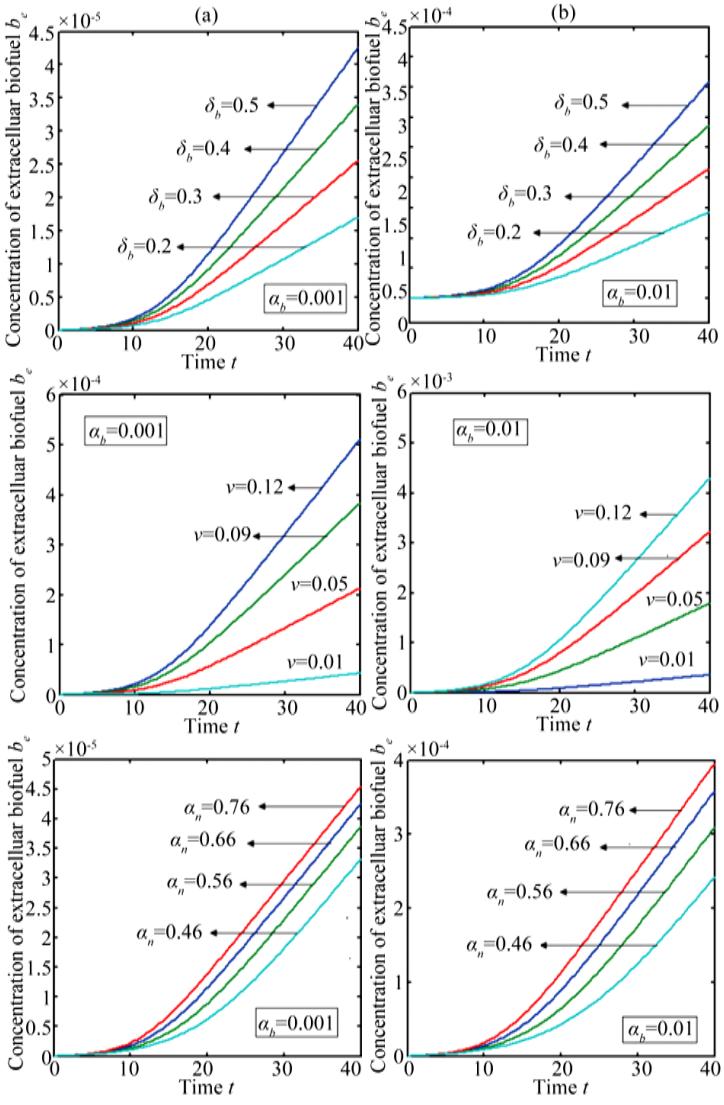

Figure 6. Concentration of extracellular biofuel $b_e(t)$ versus time t for various values of biofuel export rate per pump δ_b, ratio of intra to extracellular volume ν and cell growth rate α_n and for some fixed values of the parameters (refer **Table 1**).

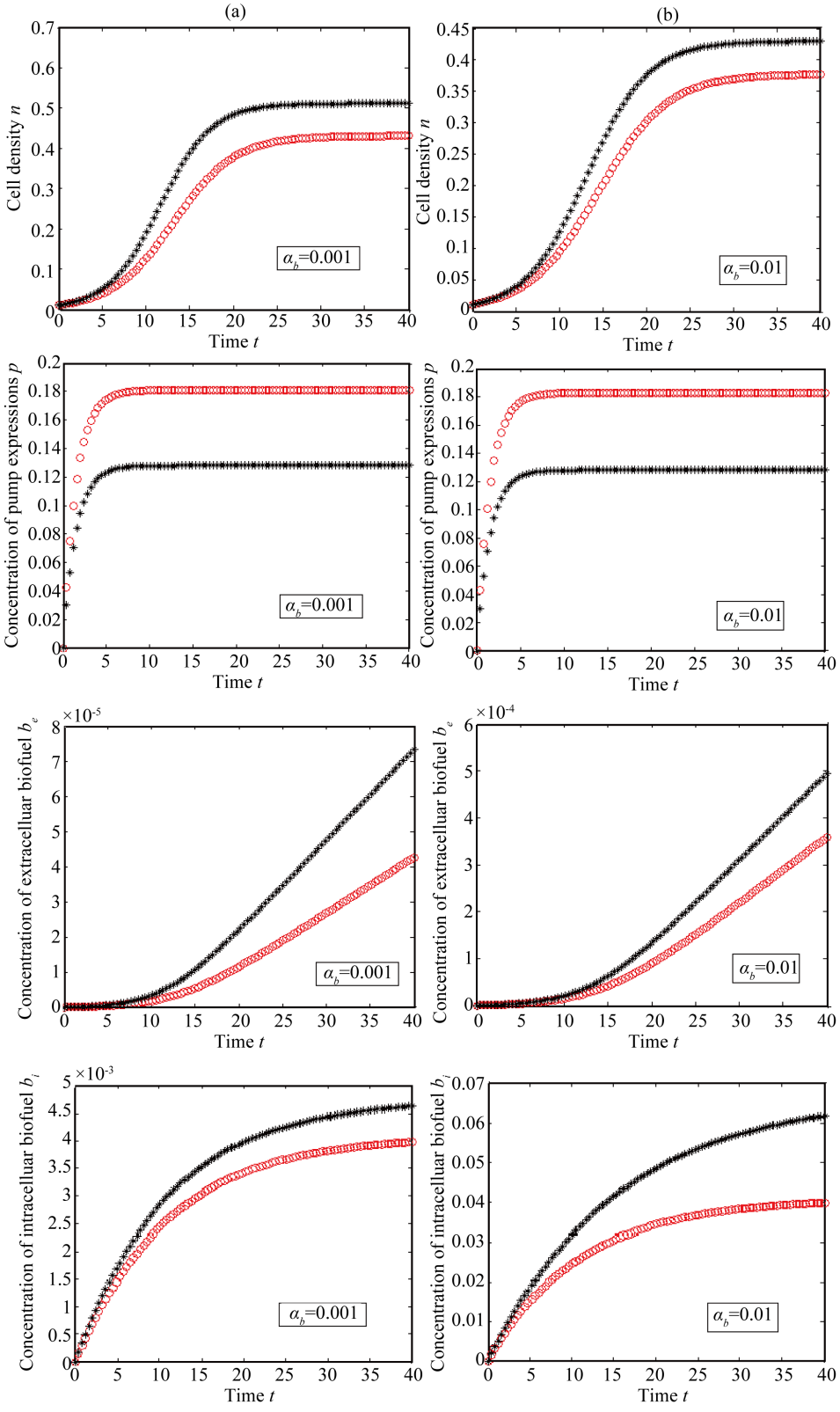

Figure 7. Comparision of concentrations for feedback (Equations (11)-(15)) and constant pump model (Equations (21)-(24)) for various values of biofuel production rate. The key to the graph: "***" represents the constant pump model and "ooo" represents the feedback model.

shows that the feedback model is better suited then constant pump for all values of the parameter. Also the biofuel produced for feedback model higher than constant pump model.

5. Conclusion

A time dependent non-linear differential equation in feedback and constant pump models has been solved analytically. By comparing both models analytically, the feedback model produces more biofuel than the constant pump model. For all biofuel production rates, the most highly induced sensor model produces the most biofuel. This theoretical result helps determine the various biofuel potential by changing the biofuel production rate and toxicity coefficient. The feedback control model represents a valuable contribution to synthetic biology designs for optimizing biofuel yields. This method can be extended to solve the nonlinear equations in feedback and constant pump models with diffusion term.

Acknowledgements

This work is supported by the Department of Science and Technology (DST) (No.SB/SI/PC-50/2012), Government of India, New Delhi, India. The authors are thankful to Sri. S. Natanagopal, Secretary, The Madura College Board and Dr. R. Murali, Principal, The Madura College (Autonomous), Madurai, Tamil Nadu, India for their constant encouragement. It is our pleasure to thank the editors and referees for their valuable comments.

References

[1] Singh, A., Poshtiban, S. and Eyoy, S. (2013) Recent Advances in Bacteriophage Based Biosensors for Food-Borne Pathogen Detection. *Sensors*, **13**, 1763-1786. http://dx.doi.org/10.3390/s130201763

[2] Clark, L.C. and Lyons, C. (1962) Electrode Systems for Continuous Monitoring Cardiovascular Surgery. *Annals of the New York Academy of Sciences*, **102**, 29-45. http://dx.doi.org/10.1111/j.1749-6632.1962.tb13623.x

[3] Sara, R.M., Maria, J.L. and Damia, B. (2006) Biosensors as Useful Tools for Environmental Analysis and Monitoring. *Analytical and Bioanalytical Chemistry*, **386**, 1025-1041. http://dx.doi.org/10.1007/s00216-006-0574-3

[4] Clomburg, J.M. and Gonzalez, R. (2010) Biofuel Production in *Escherichia coli*: The Role of Metabolic Engineering and Synthetic Biology. *Applied Microbiology and Biotechnology*, **86**, 419-434. http://dx.doi.org/10.1007/s00253-010-2446-1

[5] Fischer, C.R., Marcuschamer, D.K. and Stephanopoulos, G. (2008) Selection and Optimization of Microbial Hosts for Biofuels Production. *Metabolic Engineering*, **10**, 295-304. http://dx.doi.org/10.1016/j.ymben.2008.06.009

[6] Mostafa, S.E. (2010) Microbiological Aspects of Biofuel Production: Current Status and Future Directions. *Journal of Advanced Research*, **1**, 103-111. http://dx.doi.org/10.1016/j.jare.2010.03.001

[7] Peralta, P.P. and Keasling, J.D. (2010) Advanced Biofuel Production in Microbes. *Journal of Biotechnology*, **5**, 147-162. http://dx.doi.org/10.1002/biot.200900220

[8] Soto, S.M. (2013) Role of Efflux Pumps in the Antibiotic Resistance of Bacteria Embedded in a Biofilm. *Virulence*, **4**, 223-229. http://dx.doi.org/10.4161/viru.23724

[9] Huffer, S., Roche, C.M., Blanch, H.W. and Clark, D.S. (2012) *Escherichia coli* for Biofuel Production: Bridging the Gap from Promise to Practice. *Trends in Biotechnology*, **30**, 538-545. http://dx.doi.org/10.1016/j.tibtech.2012.07.002

[10] Christopher, M.G. and Stephen, S.F. (2011) Applications of Systems Biology towards Microbial Fuel Production. *Trends in Microbiology*, **19**, 10.

[11] Dunlop, M.J., Keasling, J.D. and Mukhopadhyay, A. (2010) A Model for Improving Microbial Biofuel Production Using a Synthetic Feedback Loop. *Systems and Synthetic Biology*, **4**, 95-104. http://dx.doi.org/10.1007/s11693-010-9052-5

[12] Harrison, M.E. and Dunlop, M.J. (2012) Synthetic Feedback Loop Model for Increasing Microbial Biofuel Production Using a Biosensor. *Frontiers in Microbiology*, **3**, 360. http://dx.doi.org/10.3389/fmicb.2012.00360

[13] Anitha, S., Subbiah, A., Subramaniam, S. and Rajendran, L, (2011) Analytical Solution of Amperometric Enzymatic Reactions Based on Homotopy Perturbation Method. *Electrochimica Acta*, **56**, 3345-3352. http://dx.doi.org/10.1016/j.electacta.2011.01.014

[14] Hemeda, A.A. (2012) Homotopy Perturbation Method for Solving Systems of Nonlinear Coupled Equations. *Applied Mathematical Sciences*, **6**, 4787-4800.

[15] He, J.H. (1999) Homotopy Perturbation Technique. *Computer Methods in Applied Mechanics and Engineering*, **178**,

257-262. http://dx.doi.org/10.1016/S0045-7825(99)00018-3

[16] He, J.H. (2005) Application of Homotopy Perturbation Method to Nonlinear Wave Equations. *Chaos, Solitons and Fractals*, **26**, 695-700. http://dx.doi.org/10.1016/j.chaos.2005.03.006

[17] Eswari, A., Usha, S. and Rajendran, L. (2011) Approximate Solution of Non-Linear Reaction Diffusion Equations in Homogeneous Processes Coupled to Electrode Reactions for CE Mechanism at a Spherical Electrode. *American Journal of Analytical Chemistry*, **2**, 93-103. http://dx.doi.org/10.4236/ajac.2011.22010

[18] PonRani, V.M. and Rajendran, L. (2012) Mathematical Modelling of Steady-State Concentration in Immobilized Glucose Isomerase of Packed-Bed Reactors. *Journal of Mathematical Chemistry*, **50**, 1333-1346. http://dx.doi.org/10.1007/s10910-011-9973-6

Appendix A

In this appendix, the general solutions of Equations (1)-(5) are derived. Consider the Equation (1),

$$\frac{\mathrm{d}n(t)}{\mathrm{d}t}=\alpha_n n(t)\left(1-\frac{n(t)}{n_{\max}}\right)-\delta_n b_i(t)n(t)-\frac{\alpha_n p(t)n(t)}{p(t)+\gamma_p} \tag{A1}$$

The above equation is strongly nonlinear. Hence we take $b_i = b_{is}$ and $p = p_s$. Now the Equation (A1) becomes

$$\frac{\mathrm{d}n(t)}{\mathrm{d}t}=\alpha_n n(t)\left(1-\frac{n(t)}{n_{\max}}\right)-\delta_n b_{is} n(t)-\frac{\alpha_n p_s n(t)}{p_s+\gamma_p} \tag{A2}$$

We rewrite (A2) as

$$\frac{\mathrm{d}n(t)}{\mathrm{d}t}=\left(\alpha_n-\delta_n b_{is}-\frac{\alpha_n p_s}{p_s+\gamma_p}\right)n(t)-\left(\frac{\alpha_n}{n_{\max}}\right)\left(n(t)\right)^2 \tag{A3}$$

By solving (A3), we get

$$n(t)=\frac{L}{\frac{\alpha_n}{n_{\max}}+C1(L)\mathrm{e}^{-(L)t}} \tag{A4}$$

From Equation (A4), we can find the constant C1 can be obtained by substitute the initial condition. We get

$$C1=\frac{L-\frac{n_0\alpha_n}{n_{\max}}}{n_0(L)} \tag{A5}$$

Substitute Equation (A5) in Equation (A4), the final solution is obtained.

$$n(t)=\frac{L}{\frac{\alpha_n}{n_{\max}}+\frac{1}{n_0}\left(L-\frac{n_0\alpha_n}{n_{\max}}\right)\mathrm{e}^{-Lt}} \tag{A6}$$

where $L=\left(\alpha_n-\delta_n b_{is}-\frac{\alpha_n p_s}{p_s+\gamma_p}\right)$ (A7)

When $t\to\infty$, the above equation becomes $n(t)=n_s$. (A8)

Appendix B

Scilab/Matlab program to find the numerical solution of Equations (1)-(5).

```
function main1
options= odeset('RelTol',1e-6,'Stats','on');
Xo = [0.01;0;0;0;0];
tspan = [0,40];
tic
[t,X]= ode45(@TestFunction,tspan,Xo,options);
toc
figure
holdon
plot(t, X(:,1))
%plot(t, X(:,2))
%plot(t, X(:,3))
%plot(t, X(:,4))
%plot(t, X(:,5))
```

```
return
function [dx_dt]= TestFunction(t,x)
an=0.66;ar=0.01;ap=0.01;ab=0.01;
br=2.1;bp=0.66;
dn=0.91;db=0.5;
gp=0.14;gi=60;gr=1.8;
kr=10;kp=0.2;kb=100;nmax=1;
v=0.01;i1=1;
dx_dt(1)=(an*x(1)*(1-(x(1)/nmax)))-(dn*x(4)*x(1))-(an*x(1)*x(3)/(x(3)+gp));
dx_dt(2)=ar+(kr*(i1/(i1+gi)))-(br*x(2));
dx_dt(3)=ap+(kp*(1/(gr+(x(2)/(1+(kb*x(4)))))))-(x(3)*bp);
dx_dt(4)=(ab*x(1))-(x(3)*db*x(4));
dx_dt(5)=v*db*x(3)*x(4)*x(1);
dx_dt = dx_dt';
```